ACS APPLIED MATERIALS & INTERFACES

Research Article

www.acsami.org

Controlling the Formation of Phospholipid Monolayer, Bilayer, and Intact Vesicle Layer on Graphene

Seyed R. Tabaei,[†,‡] Wei Beng Ng,[†,‡] Sang-Joon Cho,[§,∥] and Nam-Joon Cho*[,†,‡,⊥]

[†]School of Materials Science and Engineering and [‡]Centre for Biomimetic Sensor Science, Nanyang Technological University, 50 Nanyang Avenue, 639798 Singapore

[§]Research and Development Center, Park Systems, Suwon 443-270, South Korea

[∥]Advanced Institute of Convergence Technology, Seoul National University, Suwon 443-270, South Korea

[⊥]School of Chemical and Biomedical Engineering, Nanyang Technological University, 62 Nanyang Drive, 637459 Singapore

Supporting Information

ABSTRACT: Exciting progress has been made in the use of graphene for bio- and chemical sensing applications. In this regard, interfacing lipid membranes with graphene provides a high-sealing interface that is resistant to nonspecific protein adsorption and suitable for measuring biomembrane-associated interactions. However, a controllable method to form well-defined lipid bilayer coatings remains elusive, and there are varying results in the literature. Herein, we demonstrate how design strategies based on molecular self-assembly and surface chemistry can be employed to coat graphene surface with different classes of lipid membrane architectures. We characterize the self-assembly of lipid membranes on CVD-graphene using quartz crystal microbalance with dissipation, field-effect transistor, and Raman spectroscopy. By employing the solvent-assisted lipid bilayer (SALB) method, a lipid monolayer and bilayer were formed on pristine and oxygen-plasma-treated CVD-graphene, respectively. On these surfaces, vesicle fusion method resulted in formation of a lipid monolayer and intact vesicle layer, respectively. Collectively, these findings provide the basis for improved surface functionalization strategies on graphene toward bioelectronic applications.

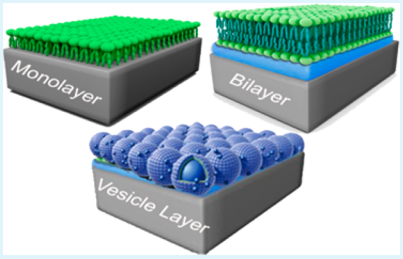

KEYWORDS: *surface coating, biofunctionalization, self-assembly, graphene, supported lipid bilayer, lipid monolayer, adsorbed vesicle layer*

INTRODUCTION

Graphene-based materials attract wide interest across the chemical sciences because of the unique electrical and mechanical properties of graphene.[1] An ongoing area of interest involves interfacing graphene with biological systems, especially for sensor applications.[2−5] For such purposes, there is great demand for fabricating lipid bilayer coatings on graphene. Such coatings can serve as biofouling-resistant layers in bioelectronics devices and can enable surface functionalization and the possibility to host membrane-associated biomolecules. Figure 1 presents three different model membrane platforms, including the supported lipid monolayer,[6−8] bilayer (SLB),[9] and adsorbed vesicle layer,[10] which can form on solid supports depending on the corresponding surface chemistry.

Although there has been some promise in fabricating lipid nanostructures, a controllable method to form well-defined lipid bilayer coatings remains elusive, and there are varying results in the literature. Early work by Ang et al.,[11] reported lipid bilayer formation on graphene by using the vesicle fusion method conducted at high temperature (60 °C), and the conclusion was based on interrogating the fluidic properties of the lipid adlayer. By contrast, Hirtz et al.,[12] reported formation of a lipid monolayer on graphene by dip-pen lithography, as confirmed by direct morphological measurements with atomic force microscopy. The discrepancies suggest that a clear understanding of why different kinds of lipid membrane architectures can form on graphene is lacking especially from the perspective of how surface chemistry and the chosen fabrication method influence the fate of the molecular self-assembly process.

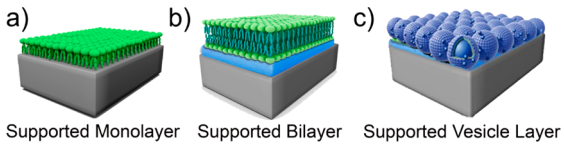

Figure 1. Schematic illustration of three model membrane systems. (a) Supported monolayer and (b) bilayer provide a natural environment for surface immobilization of membrane-associated molecules at the immediate vicinity (∼5−10 nm) of the surface and impart biocompatibility and biofunctionality to the sensor surface. (c) Intact vesicles adsorbed on a substrate can be used to study the effects of membrane curvature.

Received: March 8, 2016
Accepted: April 19, 2016
Published: April 19, 2016

DOI: 10.1021/acsami.6b02837
ACS Appl. Mater. Interfaces 2016, 8, 11875−11880

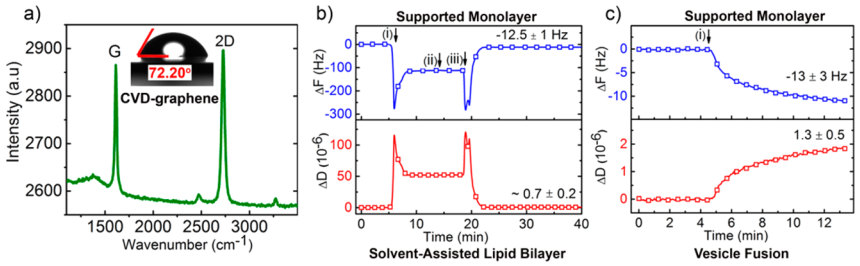

Figure 2. QCM-D analysis of lipid membrane formation on pristine CVD-graphene. (a) Representative Raman spectrum from CVD-graphene on a QCM-D crystal. Inset shows a photograph of a water droplet and the contact angle on CVD-graphene. (b) QCM-D frequency shift (ΔF, top panel) and dissipation shift (ΔD, bottom panel) for the third overtone were measured as a function of time during the formation of a lipid monolayer on a QCM-D crystal coated with CVD-graphene. The arrows indicate the injection of (i) isopropanol, (ii) lipid mixture (0.5 mg/mL of DOPC in isopropanol), and (iii) Tris buffer (10 mM Tris, 150 mM NaCl, pH 7.5), producing a final ΔF and ΔD of -12.5 ± 1 Hz and $0.7 \pm 0.2 \times 10^{-6}$, respectively. (c) QCM-D responses during the adsorption of vesicles onto CVD-graphene. DOPC vesicles were added at t = 5 min (i) after establishing the baseline for the frequency and dissipation shifts.

In the conventional vesicle fusion method, when small (<100 nm) unilamellar vesicles are added to a solid surface, they adsorb to the surface, and provided the adhesion energy between the membrane and the support is high enough, they rupture and subsequently fuse to form a continuous bilayer or monolayer on hydrophilic or hydrophobic surfaces, respectively.[13] However, if the energetics are insufficient, then the surface-adhered vesicles remain intact.[14] The energetics of the system are controlled by the lipid composition, the material properties of the support,[15] and the environmental conditions such as ionic strength,[16] solution pH,[17] and osmotic pressure.[18] The outcome is determined by a delicate balance between intermolecular interactions, i.e., van der Waals,[19] electrostatic,[20] and hydration forces.[21] Under physiological conditions, successful bilayer formation using vesicle fusion is mainly applicable to silicon-based materials such as silicon dioxide, glass, and mica. The solvent-assisted lipid bilayer (SALB)[22,23] method is an alternative membrane formation technique that does not require lipid vesicles. The method involves lipid deposition onto a solid surface in an alcohol, e.g., isopropanol, followed by gradual replacement of the alcohol by an aqueous buffer to drive self-assembly of a lipid bilayer or monolayer on hydrophilic or hydrophobic surfaces, respectively. This self-assembly pathway sidesteps vesicle rupture, which is usually the preventive stage in the transformation of vesicles to a bilayer. The SALB method has been applied successfully on a wide variety of surfaces including SiO_2, Au, Al_2O_3, and hydrophobic alkanethiol-coated gold.[22,24]

In this work, we have investigated how the surface properties of graphene affect the self-assembly of phospholipid molecules on CVD-graphene, which is known to be typically hydrophobic,[25] and compared the results with those obtained from oxygen-plasma treated graphene (denoted as O_2-graphene), which increases the surface hydrophilicity. Two fabrication strategies were chosen, the vesicle fusion and the SALB methods, and the corresponding membrane formation processes were tracked by quartz crystal microbalance with dissipation (QCM-D) monitoring. In addition, we probed the modulation of the electronic state of graphene by utilizing charged lipids, as determined by electrical measurements and Raman spectroscopy.

MATERIALS AND METHODS

Lipid Preparation. Zwitterionic lipid, 1,2-dioleoyl-*sn*-glycero-3-phosphocholine (DOPC), cationic lipid 1,2-dioleoyl-*sn*-glycero-3-ethylphosphocholine (chloride salt) (DOEPC), and anionic lipid 1,2-dioleoyl-*sn*-glycero-3-phospho-L-serine (sodium salt) (DOPS) were purchased from Avanti Polar Lipids (Alabaster, AL). To prepare the lipid samples for vesicle preparation, chloroform solutions of lipids with desired composition were first dried using a gentle stream of nitrogen gas and subsequently stored under vacuum overnight to remove traces of chloroform. Vesicles were prepared in tris buffer (10 mM Tris, 150 mM NaCl, pH 7.5) via extrusion through 50 nm diameter, track-etched polycarbonate membranes as previously described.[26] For SALB experiments, DOPC lipid powder was first dissolved in isopropanol at 10 mg/mL lipid concentration. The stock was diluted to a 0.5 mg/mL lipid concentration before experiments.

Quartz Crystal Microbalance with Dissipation (QCM-D) Monitoring. A Q-Sense E4 (Q-Sense AB, Gothenburg, Sweden) instrument was used to monitor the adsorption kinetics of lipids onto graphene-coated 5 MHz, AT-cut piezoelectric quartz crystals. The custom-made graphene-coated QCM-D crystal was obtained from Cheap Tubes Inc., Grafton, USA. Graphene was grown on copper using chemical vapor deposition (CVD) and transferred onto the SiO_2 coated QCM-D crystal (QSense AB). Changes in frequency (ΔF) and energy dissipation (ΔD) were recorded as functions of time, as previously described.[27] The measurement data was collected at the n = 3−11 overtones, and the reported values were recorded at the third overtone ($\Delta F_n = 3/3$). All samples were introduced at a flow rate of 50 μL/min using a peristaltic pump (Ismatec Reglo Digital) under continuous flow conditions. The temperature of the flow cell was fixed at 24.00 ± 0.5 °C.

Oxygen Plasma Treatment. Before experiment, sensor surfaces were treated with oxygen plasma at 5 W for 30 s (March Plasmod Plasma Etcher, March Instruments, California) immediately before use.

Raman Spectroscopy. A 488 nm excitation laser and a 100× objective lens of a confocal spectrometer (alpha 300R, WiTEC, Germany) were used for Raman spectrum collection with a laser power of <1 mW to avoid sample damage.

Contact angle. Water contact angle measurement was done at ambient laboratory temperatures using a Dataphysics OCA 15Pro instrument. The static water contact angle was measured as the angle from the tangent to the horizontal of 6 μL sessile drops of deionized water.

Field-Effect Transistor Fabrication and Measurement. Using a stainless-steel shadow mask of channel length 4000 μm and width of 2000 μm, chromium electrodes were first sputtered on the CVD graphene/SiO_2/Si substrate as an adhesion layer before the subsequent sputtering of gold on top of the chromium electrodes. The thickness of the resultant Cr/Au was about 10/100 nm serving as the source and drain. Polydimethylsiloxane (PDMS) (with 10 wt % curing agent) (Sylgard 184) was fabricated as the encapsulating fluidic chamber and assembled on top of the source and drain electrodes using precured PDMS (with 50 wt % curing agent) as an adhesion layer. After overnight drying in air at room temperature, the edges were reinforced to the substrates by air-cured epoxy glue. The PDMS

DOI: 10.1021/acsami.6b02837
ACS Appl. Mater. Interfaces 2016, 8, 11875−11880

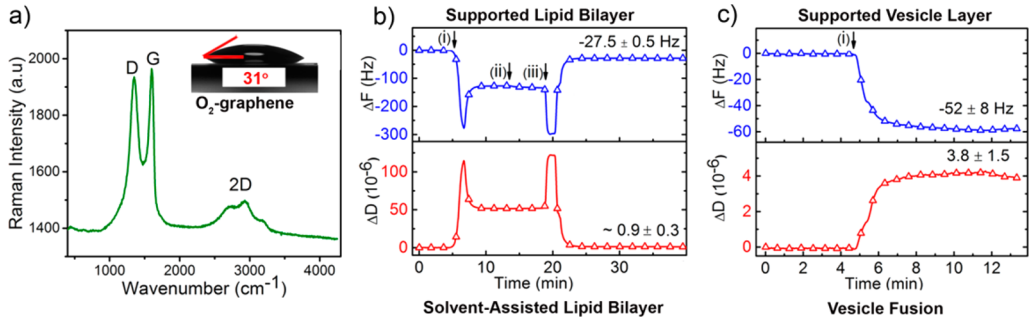

Figure 3. QCM-D analysis of lipid membrane formation on oxygen-plasma treated graphene. (a) Raman spectrum and illustration of the static water contact angle for O_2-graphene. QCM-D curves for (b) SALB formation (arrows indicate injection of (i) isopropanol, (ii) lipid mixture, and (iii) buffer.) and (c) vesicle fusion on O_2-graphene producing a final ΔF values of -27.5 ± 0.5 and $-52 \pm 8 \times 10^{-6}$ Hz, which correspond to a planar bilayer and an absorbed vesicle layer, respectively.

fluid chamber (Figure S1) is designed with an inlet and outlet to allow the continuous injection of liquid sample via tubing connection and a peristaltic pump (ISM 833). The electrical performance of the FETs was determined by measuring the standard two-probe configuration of the top-gated device's static characteristics (drain−source current I_D versus gate voltage V_G at constant drain−source voltage V_D of 0.1 V). These characteristics were measured using the Keithley 4200 Semiconductor Characterization System with an Ag/AgCl gate electrode.

RESULTS AND DISCUSSION

We first investigated the lipid self-assembly on pristine CVD-graphene. Figure 2a shows the Raman spectrum of a CVD-graphene sheet that was first grown on Cu and then transferred onto the QCM-D crystal. The negligible defect-related D band at around 1350 cm^{-1} and the sharp symmetric 2D peak at 2678 cm^{-1} indicated the high crystallinity of the CVD-graphene film. In general, the Raman spectrum of a monolayer sheet of graphene will show a 2D band approximately 2−2.5 times more intense than the G band at around 1586 cm^{-1}.[28] The intensity ratio, I_{2D}/I_G, of <2 in our spectrum suggested that the CVD graphene on a QCM-D crystal was at least a two-layer graphene sheet, rather than a monolayer.

We next examined the hydrophobicity of the CVD-graphene by conducting water contact angle (WCA) measurements. As shown in the inset of Figure 2a, a water droplet placed on top of the pristine graphene gave a static contact angle of 72.2°. Our pristine graphene was therefore slightly less hydrophobic than other graphene samples previously studied, which were reported to have WCA in the range of 87−127°.[29] In our case, the lower value was most likely due to the adsorption of air moisture and oxygen. Figure 2b represents the time course of QCM-D frequency (ΔF, top panels) and dissipation (ΔD, bottom panels) shifts during SALB formation on CVD-graphene. A typical SALB formation experiment involved baseline recording in the aqueous buffer solution, injection of the isopropanol (i), addition of lipid mixture in isopropanol (ii), and solvent exchange back into the initial buffer solution (iii). For CVD-graphene, the final frequency value after complete solvent replacement was -12.5 ± 1 Hz. It has previously been established that planar bilayer formation leads to changes in frequency of about −26 Hz.[13] Thus, the value obtained in our experiments corresponded to ∼50% of the value expected for bilayer formation, indicative of a lipid monolayer deposition,[13] as would be expected from the hydrophobic nature of CVD-graphene.[25] Similarly, for vesicle adsorption on CVD-graphene (Figure 2c), we observed a one-step monotonic kinetic behavior that resembled a monolayer lipid assembly with a final frequency shift of 13 ± 3 Hz. However, the relatively high standard deviation (3 Hz) suggested that the adlayer was not homogeneous. In addition, the dissipation value obtained upon vesicle fusion on CVD-graphene ($1.3 \pm 0.5 \times 10^{-6}$) was relatively high.

Next, to investigate further the self-assembly of phospholipids, we treated the CVD-graphene surface with oxygen plasma (5 W for 30 s) and compared the results of two self-assembly processes: the SALB formation method and the VF method. Upon treating the CVD graphene with oxygen plasma (denoted as O_2-graphene), there was a sharp decrease in the 2D peak intensity along with extensive peak broadening (Figure 3a). The appearance of the prominent D peak at approximately 1350 cm^{-1} confirmed the oxidation of graphene to mainly graphene oxide, which typically has a much higher proportion of structural defects. When the sample was mildly treated with oxygen plasma, the contact angle of the water droplet decreased to 31° (see the inset of Figure 3a) on O_2-graphene, which corresponded well to the range of 30−60° reported in the literature.[30] The oxidation of graphene induces the formation of epoxides and hydroxyl groups on the basal plane and of carboxyl groups at the edges of the graphene sheets.[30] In particular, defective sites containing hydroxyl groups are mainly responsible for the hydrophilic nature of graphene oxide.

To follow the assembly of lipid bilayer, a typical QCM-D response was measured for the SALB formation on O_2-graphene as shown in Figure 3b. Once the SALB procedure was completed as previously described, the ΔF values were consistent with previous QCM-D responses for planar lipid bilayer formation (-27.5 ± 0.5 Hz), and the energy dissipation ($0.9 \pm 0.3 \times 10^{-6}$) was acceptable for a homogeneous and defect-free bilayer ($<0.5 \times 10^{-6}$). These results suggest that the SALB formation method is necessary and sufficient to form a planar lipid bilayer on an O_2-graphene surface. In marked contrast, the addition of vesicles onto the O_2-graphene caused the frequency to decrease and dissipation to increase monotonically until they reached the final values of -52 ± 8 and $3.8 \pm 1.5 \times 10^{-6}$ Hz respectively. When adsorbed vesicles remain intact on the surface forming a vesicular layer, a significant quantity of water is trapped inside as well as between the adsorbed vesicles, which is detected as a mass gain by the QCM-D frequency signal, and this additional hydrodynamically coupled solvent mass dissipates a large amount of energy. Therefore, the QCM-D measurement results indicate that adsorbed vesicles did not rupture and remained intact on O_2-graphene. Our results agreed well with a related study by

DOI: 10.1021/acsami.6b02837
ACS Appl. Mater. Interfaces 2016, 8, 11875−11880

Okamoto et al.,[31] which demonstrated that, vesicles remain intact on graphene oxide in the absence of Ca^{2+} ion. These data therefore indicate that O_2-graphene can support a layer of intact vesicles.

The electrical response of atomically thin CVD-graphene to charged molecules at the interface provides a sensitive modality for the detection of biomolecular binding. To characterize the electronic effect of charged lipids, we measured the electrical response of the lipid monolayer on a CVD-graphene sheet, fabricated as a three-terminal field-effect transistor (FET) (Figure 4a,b). Monolayers of different charges were prepared

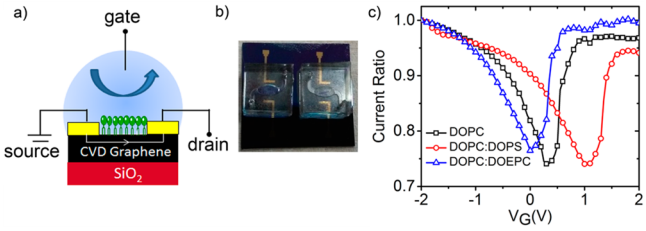

Figure 4. Electrical measurement of lipid-coated graphene. (a) Schematics of a lipid-coated graphene in liquid-gated FET device. (b) Photograph of polydimethylsiloxane (PDMS) microfluidic device with integrated electrodes. (c) IV curves for three-terminal field effect transistor (FET) graphene coated with zwitterionic DOPC (rectangles), positively charged DOPC:DOEPC (20%) (triangles), and negatively charged DOPC:DOPS (20%) (circles) monolayers formed by vesicle fusion.

by the vesicle fusion method, and the drain−source current (I_{DS}) was measured as a function of gate bias (V_G). As shown in Figure 4c, the characteristic V-shaped curve, indicating the Dirac point of graphene, was retained when neutral and charged lipids were coated on the graphene. A noticeable difference was the shifting of the Dirac point upon lipid adsorption. The Dirac point shifted toward negative gate voltage when positively charged DOPC:DOEPC (4:1) monolayer was formed; conversely, it shifted toward positive gate voltage when a positively charged DOPC:DOPS (4:1) was coated. The observed voltage shift due to the charged lipids corresponded well with the trend observed by Ang et al.[11] and was a consequence of the charge-impurity potential generated by the charged membranes atop the CVD-graphene. The shift in the electrically neutral Dirac point was a direct manifestation of the modulations of the hole and electron concentrations in the graphene; these modulations were induced by the charged membranes via a field effect across the ultrathin water interlayer between the lipid membranes and the graphene. It should be noted that the Dirac point upon the formation of a neutral lipid membrane was slightly positive at +0.4 V because of the presence of negatively charged impurities trapped on the surface of the SiO_2/Si substrate. In addition, the magnitude of the Dirac point shift in the presence of negatively charged lipids was larger than that in the presence of positively charged lipids for the same concentration of net lipid charge. It is possible that the positively charged lipids induced a partial nullification of the impurity potential generated by the underlying negatively charged surface impurities on the SiO_2/Si substrate.

We further measured the influence of lipid membrane formation on graphene using Raman spectroscopy. Figure 5a shows a representative Raman spectrum for DOPC bilayer on silicon dioxide. Consistent with previous reports,[32] an intense C−H stretching band appeared at 2871 cm^{-1} even though the symmetric and asymmetric components of C−H stretching were not resolved. On CVD-graphene, prominent peaks corresponding to the different molecular vibration modes of C−C and C−H bonds in the neutral DOPC monolayer were clearly identified in comparison to the characteristic G and 2D peaks of graphene, as shown in Figure 5b.

Interestingly, the symmetric and asymmetric components of C−H stretching were resolved on graphene. Raman spectroscopy was repeated on graphene coated with positively charged DOPC:DOEPC (4:1) and negatively charged DOPC:DOPS (4:1) monolayers. Upon closer examination of the 2D peaks in Figure 5c, a shift in the wavenumber was detected for the charged lipids. Although positively charged lipids induced an upward shift, i.e., a higher wavenumber for the 2D peaks, negatively charged lipids displayed a downward shift.

The Raman shift could be explained as the n and p doping effects of the negatively and positively charged lipids, respectively, on graphene.[12] The Raman results supported the charge-impurity potential effect of the charged lipids, which was demonstrated in the Dirac point shift in the I_{DS}−V_G measurement shown in Figure 4c. Interestingly, the magnitude of the Raman peak shift was smaller for the positively charged lipids than it was for the negatively charged lipids. The unbalanced shift magnitude again reflected the same observation from the I_{DS}−V_G curves, which can be attributed to the presence of surface charges from impurities on the SiO_2/Si substrate. Das et al.[33] performed in situ Raman measurements on a graphene transistor, and on the basis of density function theory (DFT) and experimental measurements, they correlated the position of the 2D peak to the doping level. Using their calibration (see Figure 3 of ref 33 for the position of the 2D peak as a function of doping), the Raman shift in our measurement (2688 cm^{-1} for DOPC:DOPS) corresponded to a change in the carrier density of ~3 × 10^{13} cm^{-2}. Considering that each phospholipid occupies a 0.68 nm^2 surface area[34] and

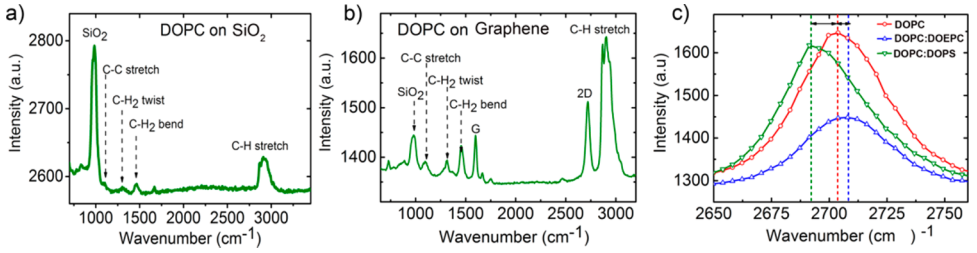

Figure 5. Raman spectroscopy analysis of lipid membrane formation on graphene. Raman spectra with band assignments for a DOPC bilayer on (a) SiO_2 and (b) CVD-graphene. (c) Raman spectra of CVD-graphene coated with lipid monolayers of different charge, showing the shift of the 2D peak.

DOI: 10.1021/acsami.6b02837
ACS Appl. Mater. Interfaces 2016, 8, 11875−11880

noting that 20% of the surface groups are charged, the estimated value of this impurity charge density was ~2.86 × 10^{13} cm^{-2}, which was in good agreement with the calculated charge density. These results also further supported the formation of a lipid monolayer, rather than a bilayer, on the hydrophobic graphene. Taken together, both vesicle fusion and SALB result in formation of a lipid monolayer on the hydrophobic pristine CVD-graphene. On the hydrophilic oxygen-plasma-treated graphene (O_2-graphene), SALB and vesicle fusion resulted in formation of a bilayer and intact vesicle layer, respectively.

CONCLUSIONS

QCM-D was for the first time used to monitor lipid self-assembly on a graphene surface. The characterization of lipid attachment on graphene demonstrates that depending on the preparation condition CVD-graphene can support the formation of a lipid monolayer, a lipid bilayer, or intact vesicles. Such capabilities provide a sensitive bioelectronic interface that is also biocompatible and antifouling. In addition, the significant modulation of the electronic properties of graphene by charged lipid membranes indicates the huge potential of using a lipid−graphene interface as an ultrasensitive platform for sensing membrane-related processes, using Raman spectroscopy and electronic measurements.

ASSOCIATED CONTENT

Supporting Information

The Supporting Information is available free of charge on the ACS Publications website at DOI: 10.1021/acsami.6b02837.

Photographs of polydimethylsiloxane (PDMS) microfluidic device with integrated electrodes (left) and the chamber in its assembled form. (PDF)

AUTHOR INFORMATION

Corresponding Author

*E-mail: njcho@ntu.edu.sg.

Notes

The authors declare no competing financial interest.

ACKNOWLEDGMENTS

This work was supported by the National Research Foundation (NRF-NRFF2011-01).

REFERENCES

(1) Huang, X.; Yin, Z.; Wu, S.; Qi, X.; He, Q.; Zhang, Q.; Yan, Q.; Boey, F.; Zhang, H. Graphene-Based Materials: Synthesis, Characterization, Properties, and Applications. *Small* **2011**, *7* (14), 1876−1902.

(2) Sanchez, V. C.; Jachak, A.; Hurt, R. H.; Kane, A. B. Biological Interactions of Graphene-Family Nanomaterials: An Interdisciplinary Review. *Chem. Res. Toxicol.* **2012**, *25* (1), 15−34.

(3) Nikoleli, G. P.; Israr, M. Q.; Tzamtzis, N.; Nikolelis, D. P.; Willander, M.; Psaroudakis, N. Structural Characterization of Graphene Nanosheets for Miniaturization of Potentiometric Urea Lipid Film Based Biosensors. *Electroanalysis* **2012**, *24* (6), 1285−1295.

(4) Lee, Y. K.; Lee, H.; Nam, J.-M. Lipid-Nanostructure Hybrids and Their Applications in Nanobiotechnology. *NPG Asia Mater.* **2013**, *5* (5), e48.

(5) Wang, Y. Y.; Pham, T. D.; Zand, K.; Li, J.; Burke, P. J. Charging the Quantum Capacitance of Graphene with a Single Biological Ion Channel. *ACS Nano* **2014**, *8* (5), 4228−4238.

(6) Katagiri, K.; Hamasaki, R.; Ariga, K.; Kikuchi, J.-i. Layered Paving of Vesicular Nanoparticles Formed with Cerasome as a Bioinspired Organic−Inorganic Hybrid. *J. Am. Chem. Soc.* **2002**, *124* (27), 7892−7893.

(7) Katagiri, K.; Hamasaki, R.; Ariga, K.; Kikuchi, J.-i. Layer-by-Layer Self-Assembling of Liposomal Nanohybrid "Cerasome" on Substrates. *Langmuir* **2002**, *18* (17), 6709−6711.

(8) Czolkos, I.; Jesorka, A.; Orwar, O. Molecular Phospholipid Films on Solid Supports. *Soft Matter* **2011**, *7* (10), 4562−4576.

(9) Cho, N.-J.; Frank, C. W.; Kasemo, B.; Höök, F. Quartz Crystal Microbalance with Dissipation Monitoring of Supported Lipid Bilayers on Various Substrates. *Nat. Protoc.* **2010**, *5* (6), 1096−1106.

(10) Jung, H.; Kim, J.; Park, J.; Lee, S.; Lee, H.; Kuboi, R.; Kawai, T. Atomic Force Microscopy Observation of Highly Arrayed Phospholipid Bilayer Vesicle on a Gold Surface. *J. Biosci. Bioeng.* **2006**, *102* (1), 28−33.

(11) Ang, P. K.; Jaiswal, M.; Lim, C. H. Y. X.; Wang, Y.; Sankaran, J.; Li, A.; Lim, C. T.; Wohland, T.; Barbaros, O.; Loh, K. P. A Bioelectronic Platform Using a Graphene-Lipid Bilayer Interface. *ACS Nano* **2010**, *4* (12), 7387−7394.

(12) Hirtz, M.; Oikonomou, A.; Georgiou, T.; Fuchs, H.; Vijayaraghavan, A. Multiplexed Biomimetic Lipid Membranes on Graphene by Dip-Pen Nanolithography. *Nat. Commun.* **2013**, *4*, 2591.

(13) Keller, C.; Kasemo, B. Surface Specific Kinetics of Lipid Vesicle Adsorption Measured with a Quartz Crystal Microbalance. *Biophys. J.* **1998**, *75* (3), 1397−1402.

(14) Mager, M. D.; Almquist, B.; Melosh, N. A. Formation and Characterization of Fluid Lipid Bilayers on Alumina. *Langmuir* **2008**, *24* (22), 12734−12737.

(15) Reimhult, E.; Hook, F.; Kasemo, B. Intact Vesicle Adsorption and Supported Biomembrane Formation from Vesicles in Solution: Influence of Surface Chemistry, Vesicle Size, Temperature, and Osmotic Pressure. *Langmuir* **2003**, *19* (5), 1681−1691.

(16) Boudard, S.; Seantier, B.; Breffa, C.; Decher, G.; Felix, O. Controlling the Pathway of Formation of Supported Lipid Bilayers of Dmpc by Varying the Sodium Chloride Concentration. *Thin Solid Films* **2006**, *495* (1−2), 246−251.

(17) Cho, N.-J.; Jackman, J. A.; Liu, M.; Frank, C. W. Ph-Driven Assembly of Various Supported Lipid Platforms: A Comparative Study on Silicon Oxide and Titanium Oxide. *Langmuir* **2011**, *27* (7), 3739−3748.

(18) Jackman, J. A.; Choi, J.-H.; Zhdanov, V. P.; Cho, N.-J. Influence of Osmotic Pressure on Adhesion of Lipid Vesicles to Solid Supports. *Langmuir* **2013**, *29* (36), 11375−11384.

(19) Tero, R.; Ujihara, T.; Urisu, T. Lipid Bilayer Membrane with Atomic Step Structure: Supported Bilayer on a Step-and-Terrace Tio2 (100) Surface. *Langmuir* **2008**, *24* (20), 11567−11576.

(20) Cha, T.; Guo, A.; Zhu, X.-Y. Formation of Supported Phospholipid Bilayers on Molecular Surfaces: Role of Surface Charge Density and Electrostatic Interaction. *Biophys. J.* **2006**, *90* (4), 1270−1274.

(21) Jackman, J. A.; Zan, G. H.; Zhao, Z.; Cho, N.-J. Contribution of the Hydration Force to Vesicle Adhesion on Titanium Oxide. *Langmuir* **2014**, *30* (19), 5368−5372.

(22) Tabaei, S. R.; Choi, J.-H.; Haw Zan, G.; Zhdanov, V. P.; Cho, N.-J. Solvent-Assisted Lipid Bilayer Formation on Silicon Dioxide and Gold. *Langmuir* **2014**, *30* (34), 10363−10373.

(23) Tabaei, S. R.; Jackman, J. A.; Kim, S.-O.; Zhdanov, V. P.; Cho, N.-J. Solvent-Assisted Lipid Self-Assembly at Hydrophilic Surfaces: Factors Influencing the Formation of Supported Membranes. *Langmuir* **2015**, *31* (10), 3125−3134.

(24) Jackman, J. A.; Tabaei, S. R.; Zhao, Z.; Yorulmaz, S.; Cho, N.-J. Self-Assembly Formation of Lipid Bilayer Coatings on Bare Aluminum Oxide: Overcoming the Force of Interfacial Water. *ACS Appl. Mater. Interfaces* **2015**, *7* (1), 959−968.

(25) Leenaerts, O.; Partoens, B.; Peeters, F. Water on Graphene: Hydrophobicity and Dipole Moment Using Density Functional Theory. *Phys. Rev. B: Condens. Matter Mater. Phys.* **2009**, *79* (23), 235440.

(26) MacDonald, R. C.; MacDonald, R. I.; Menco, B. P. M.; Takeshita, K.; Subbarao, N. K.; Hu, L.-r. Small-Volume Extrusion

DOI: 10.1021/acsami.6b02837
ACS Appl. Mater. Interfaces 2016, 8, 11875−11880

Apparatus for Preparation of Large, Unilamellar Vesicles. *Biochim. Biophys. Acta, Biomembr.* **1991**, *1061* (2), 297−303.
(27) Rodahl, M.; Höök, F.; Fredriksson, C.; Keller, C. A.; Krozer, A.; Brzezinski, P.; Voinova, M.; Kasemo, B. Simultaneous Frequency and Dissipation Factor Qcm Measurements of Biomolecular Adsorption and Cell Adhesion. *Faraday Discuss.* **1997**, *107*, 229−246.
(28) Ferrari, A. C.; Basko, D. M. Raman Spectroscopy as a Versatile Tool for Studying the Properties of Graphene. *Nat. Nanotechnol.* **2013**, *8* (4), 235−246.
(29) Rafiee, J.; Mi, X.; Gullapalli, H.; Thomas, A. V.; Yavari, F.; Shi, Y.; Ajayan, P. M.; Koratkar, N. A. Wetting Transparency of Graphene. *Nat. Mater.* **2012**, *11* (3), 217−222.
(30) Wei, N.; Peng, X.; Xu, Z. Understanding Water Permeation in Graphene Oxide Membranes. *ACS Appl. Mater. Interfaces* **2014**, *6* (8), 5877−5883.
(31) Okamoto, Y.; Tsuzuki, K.; Iwasa, S.; Ishikawa, R.; Sandhu, A.; Tero, R.; Sandhu, A. Fabrication of Supported Lipid Bilayer on Graphene Oxide. *Asia-Pacific Interdisciplinary Research Conference 2011* **2012**, *352*, 012017.
(32) Ahmed, S.; Nikolov, Z.; Wunder, S. L. Effect of Curvature on Nanoparticle Supported Lipid Bilayers Investigated by Raman Spectroscopy. *J. Phys. Chem. B* **2011**, *115* (45), 13181−13190.
(33) Das, A.; Pisana, S.; Chakraborty, B.; Piscanec, S.; Saha, S. K.; Waghmare, U. V.; Novoselov, K. S.; Krishnamurthy, H. R.; Geim, A. K.; Ferrari, A. C.; Sood, A. K. Monitoring Dopants by Raman Scattering in an Electrochemically Top-Gated Graphene Transistor. *Nat. Nanotechnol.* **2008**, *3* (4), 210−215.
(34) Kučerka, N.; Tristram-Nagle, S.; Nagle, J. F. Structure of Fully Hydrated Fluid Phase Lipid Bilayers with Monounsaturated Chains. *J. Membr. Biol.* **2006**, *208* (3), 193−202.

DOI: 10.1021/acsami.6b02837
ACS Appl. Mater. Interfaces 2016, 8, 11875−11880